

MODELS FOR UWB PULSES AND THEIR EFFECTS ON NARROWBAND DIRECT CONVERSION RECEIVERS

Leonard E. Miller
Wireless Communication Technologies Group
National Institute of Standards and Technology
Gaithersburg, Maryland
LMiller@antd.nist.gov

ABSTRACT

A methodology is shown for predicting the effect of pulsed UWB communication waveforms on direct conversion quadrature (I/Q) receivers at baseband by analysis or simulation, making use of mathematical models of UWB pulses, of which several examples are given. The unique characteristics of UWB pulses are used to derive predictions of the UWB interference at baseband using both time- and frequency-domain calculations of the baseband filter's response to the pulses. The final result of this analysis is an estimate of the rise in receiver noise level due to the UWB interference.

1. INTRODUCTION

Along with the proliferation of wireless devices of all kinds has come a demand for higher throughput, which has generated interest in using UWB signaling techniques and waveforms because of their bandwidth. Also, interest is growing in the potential for combined communications and localization using UWB as well [1], leading to FCC approval of the use of UWB communication devices between 3.1 and 10.6 GHz under certain emission restrictions [2].

Inevitably the question of the coexistence of UWB devices with other, conventional systems arises, since the bandwidth occupied by a UWB pulse can span portions of the spectrum presently allotted to various conventional radio services. In this paper, a framework is given for modeling the effect of a hypothetical UWB signal on the baseband output of a direct conversion (I/Q) receiver within the bandwidth of the UWB signal.

2. MODELS FOR UWB SIGNALS

Perhaps the simplest UWB communication pulse waveform is the monopulse, an example of which is plotted in Figure 1. Although it is an idealized waveform, it does serve to illustrate the important distinction that must be made between transmitted and received pulsed UWB waveforms, a distinction that is necessary because the effect of the transmitting and receiving

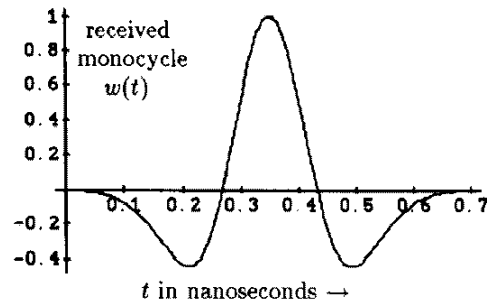


Figure 1. Monopulse UWB waveform (from [3])

antennas on the shape of the waveform as a function of time is very noticeable, unlike the case of longer duration waveforms using carriers. Regarding the physical generation of UWB waveforms, it is sufficient to note that the transmitting antenna has the general effect of differentiating the time waveform presented to it. As a consequence the transmitted pulse does not have a DC (direct current) value—the integral of the waveform over its duration must equal zero. The pulse in Figure 1 satisfies this condition and therefore is a plausible model for a UWB waveform.

A clear example of how the antennas affect the UWB waveform is given in Figure 2, in which a monopulse-like pulse is differentiated twice before being received. Also shown is the reception of multi-

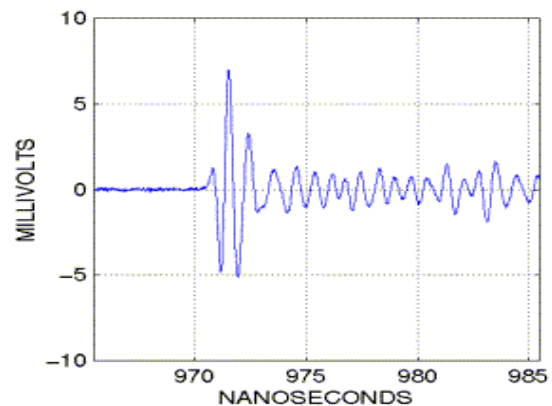


Figure 2. Example of the effect of antennas on the UWB pulse shape (from [4])

path components, a typical feature of received UWB signals.

For analysis purposes, various idealized models and generalizations of transmitted UWB pulse waveforms have been developed, including sinusoidal bursts with various envelopes (representing multiple differentiations of a monopulse, e.g.), and pulses based on Hermite polynomials [5, 6]. Assuming a communication system based on modulating successive UWB pulses, we postulate the following UWB signal:

$$z(t) = A_T \sum_{l=-\infty}^{\infty} u_l g(t - lT_u) \quad (1)$$

where A_T is a transmission gain, T_u is the pulse repetition period, the data $\{u_l\}$ are assumed to be independent, zero-mean random variables, and the pulse $g(t)$ is a UWB pulse. For the assumed modulation, the spectrum of this cyclostationary signal [7] is that for a single UWB pulse, multiplied by a factor. Note that if the data values $\{u_l\}$ are not random and zero-mean, there is a periodic component of the UWB signal, leading to lines in its spectrum.

Let the Fourier transform of the pulse $g(t)$ in (1) be denoted $G(\omega)$. For models of UWB pulses involving sinusoidal bursts with various pulse envelopes, $V(t)$, Table 1 gives the spectrum, $|G(\omega)|^2$, and autocorrelation functions, as well as noise bandwidth B_N and 3-dB bandwidth B_3 .

3. OUTPUTS OF AN I/Q RECEIVER

For an I/Q baseband receiver, the incoming signal $r(t)$ is subject to zonal bandpass filtering, then I and Q quadrature heterodyning to baseband using lowpass filters with impulse response $h_0(t)$ to extract the I and Q components of the signal, respectively. Thus, ignoring the zonal filtering and using an asterisk (*) to denote convolution, the receiver outputs are

$$I(t) = [r(t) \times \cos(\omega_c t + \varphi)] * h_0(t) \quad (2a)$$

$$Q(t) = [r(t) \times (-\sin(\omega_c t + \varphi))] * h_0(t) \quad (2b)$$

where φ is an oscillator random initial phase. The Fourier transforms of the quadrature components are

$$I(\omega) = \frac{1}{2} [e^{j\varphi} R(\omega - \omega_c) + e^{-j\varphi} R(\omega + \omega_c)] H_0(\omega) \quad (3a)$$

$$Q(\omega) = \frac{j}{2} [e^{j\varphi} R(\omega - \omega_c) - e^{-j\varphi} R(\omega + \omega_c)] H_0(\omega) \quad (3b)$$

where $R(\omega)$ is the Fourier transform of the received waveform. For example, assuming $H_0(-\omega) = H_0(\omega)$ and $H_0(\omega_1 + \omega_c) \approx 0$, if the received waveform is a sinusoid $r(t) = A \cos(\omega_1 t + \varphi)$ at frequency $f_1 = \omega_1/2\pi$, the transforms of the quadrature components are

$$I(\omega) \approx \frac{A}{4} [e^{-j\varphi} \delta(\omega + \omega_1 - \omega_c) + e^{j\varphi} \delta(\omega - \omega_1 + \omega_c)] \\ \times H_0(\omega_1 - \omega_c)$$

$$\Leftrightarrow I(t) = \frac{A}{2} H_0(\omega_1 - \omega_c) \cos[(\omega_1 - \omega_c)t + \varphi]$$

$$Q(\omega) \approx \frac{A}{4j} [e^{j\varphi} \delta(\omega - \omega_1 + \omega_c) - e^{-j\varphi} \delta(\omega + \omega_1 - \omega_c)] \\ \times H_0(\omega_1 - \omega_c)$$

$$\Leftrightarrow Q(t) = \frac{A}{2} H_0(\omega_1 - \omega_c) \sin[(\omega_1 - \omega_c)t + \varphi]$$

Thus, for a sinusoidal signal, the I and Q receiver outputs are sinusoids and can be related very simply to the parameters of the receiver filter. However, when the incoming signal has a very wide bandwidth, in general the full expressions in (2) and (3) must be used for analysis.

4. FREQUENCY AND TIME DOMAIN RESPONSES TO UWB PULSE

Taking the inverse Fourier transform of (2a) with $r(t) = g(t)$, we have the in-phase quadrature component of a received UWB pulse at baseband given by

$$p_I(t) = \frac{1}{2\pi} \int_{-\pi B}^{\pi B} d\omega e^{j\omega t} \left\{ \frac{1}{2} [e^{j\varphi} G(\omega - \omega_c) + e^{-j\varphi} G(\omega + \omega_c)] H_0(\omega) \right\} \quad (4)$$

where the range of integration is determined by the baseband filter bandwidth, B . For $B \ll \omega_c/2\pi$, the expression in the brackets is practically equal to its value for $\omega = 0$, so the in-phase quadrature component evaluates to

$$p_I(t) \doteq \frac{1}{2} [e^{j\varphi} G(-\omega_c) + e^{-j\varphi} G(\omega_c)] \\ \times \frac{1}{2\pi} \int_{-\pi B}^{\pi B} d\omega e^{j\omega t} H_0(\omega) \\ = \text{Re} \{ e^{-j\varphi} G(\omega_c) \} h_0(t) \quad (5)$$

For example, if the UWB pulse is modeled by an N -cycle sinusoid with a rectangular envelope, the in-phase response is given by

$$p_I(t) \doteq \frac{2 \sin(N\omega_c T/2 + \varphi) \sin(N\omega_c T/2)}{\omega_r [1 - (\omega_c/\omega_r)^2]} h_0(t) \quad (6)$$

Similarly, based on (2b), the cross-quadrature component is formulated as

Table 1. Spectra and autocorrelation functions for UWB pulse waveform models.

Envelope	Fine structure	Duration, bandwidth	$ G(\omega) ^2$	Autocorrelation
Rectangle: $V(t) = 1$	$\sin(\omega_r t)$, $\omega_r = 2\pi/T$	$0 \leq t \leq NT$ $B_N = \frac{1}{NT}$ $B_3 = \frac{0.886}{NT}$	$\left \frac{jT}{\pi} e^{-j\omega NT/2} \frac{\sin(\omega NT/2)}{1 - (\omega/\omega_r)^2} \right ^2$, $2N$ even $\left \frac{T}{\pi} e^{-j\omega NT/2} \frac{\cos(\omega NT/2)}{1 - (\omega/\omega_r)^2} \right ^2$, $2N$ odd	$(NT - \tau) \cdot \frac{1}{2} \cos(\omega_r \tau)$ $+ \frac{\cos(2\pi N)}{2\omega_r} \sin[\omega_r (NT - \tau)]$, $ \tau \leq NT$
Triangle: $V(t) = \frac{4}{NT} [tu(t) - 2(t - \frac{NT}{2})u(t - \frac{NT}{2}) + (t - NT)u(t - NT)]$	Noncoherent sinusoid, $\omega = \omega_r$	$0 \leq t \leq NT$ $B_N = \frac{4}{3} \frac{\omega_r}{2\pi N}$ $B_3 = 1.276 \frac{\omega_r}{2\pi N}$	$\frac{(NT)^2}{4} \left[\text{sinc}^4\left(\frac{\omega - \omega_r}{4\pi} NT\right) + \text{sinc}^4\left(\frac{\omega + \omega_r}{4\pi} NT\right) \right]$	$R_V(\tau) \cdot \frac{1}{2} \cos(\omega_r \tau)$, $R_V(\tau) =$ $\begin{cases} NT \left(\frac{4}{3} - 8\alpha^2 + 8\alpha^3 \right), & \alpha \leq \frac{1}{2} \\ 8NT \frac{(1-\alpha)^3}{3}, & \frac{1}{2} \leq \alpha \leq 1 \end{cases}$ $\alpha = \tau /NT$
Rectified Cosine: $\cos(\omega_e t)$	Noncoherent sinusoid, $\omega = \omega_r$ $= 2N\omega_e$	$ \tau \leq \pi/2\omega_e$ $B_N = \frac{\pi^2}{8} \frac{\omega_r}{2\pi N}$ $B_3 = 1.189 \frac{\omega_r}{2\pi N}$	$\frac{T^2}{16N^2\pi^2} \cos^2\left(\frac{\omega}{\omega_r} N\pi\right) \left\{ \left[\left(\frac{\omega}{\omega_r} + 1\right)^2 - \frac{1}{4N^2} \right]^{-2} + \left[\left(\frac{\omega}{\omega_r} - 1\right)^2 - \frac{1}{4N^2} \right]^{-2} \right\}$	$R_V(\tau) \cdot \frac{1}{2} \cos(\omega_r \tau)$, $R_V(\tau) = \frac{1}{2} \left(\frac{\pi}{\omega_e} - \tau \right) \cos(\omega_e \tau)$ $+ \frac{\sin(\omega_e \tau)}{2\omega_e}$, $ \tau \leq \pi/\omega_e$
Gaussian: e^{-at^2}	Noncoherent sinusoid, $\omega = \omega_r$	$B_N = \sqrt{a/2\pi}$ $B_3 = \frac{\sqrt{a(2\ln 2)}}{\pi}$	$\frac{\pi}{4a} \left[e^{-(\omega - \omega_r)^2/2a} + e^{-(\omega + \omega_r)^2/2a} \right]$	$R_V(\tau) \cdot \frac{1}{2} \cos(\omega_r \tau)$, $R_V(\tau) = \exp\left\{-\frac{a\tau^2}{2}\right\} \sqrt{\frac{\pi}{2a}}$

$$p_Q(t) = \frac{1}{2\pi} \int_{-\pi B}^{\pi B} d\omega e^{j\omega t} \left\{ \frac{j}{2} \left[e^{j\varphi} G(\omega - \omega_c) - e^{-j\varphi} G(\omega + \omega_c) \right] H_0(\omega) \right\} \quad (7)$$

For $B \ll \omega_c / 2\pi$, the expression in the brackets is practically equal to its value for $\omega = 0$, so the cross-quadrature component evaluates to

$$p_Q(t) \doteq \frac{j}{2} \left[e^{j\varphi} G(-\omega_c) - e^{-j\varphi} G(\omega_c) \right] \times \frac{1}{2\pi} \int_{-\pi B}^{\pi B} d\omega e^{j\omega t} H_0(\omega) = \text{Im} \left\{ e^{-j\varphi} G(\omega_c) \right\} h_0(t) \quad (8)$$

For example, if the UWB pulse is modeled by an N -cycle sinusoid with a rectangular envelope, the in-phase response is given by

$$p_Q(t) \doteq \frac{2 \cos(N\omega_c T / 2 + \varphi) \sin(N\omega_c T / 2)}{\omega_r \left[1 - (\omega_c / \omega_r)^2 \right]} h_0(t) \quad (9)$$

Now we consider the response of the receiver to the UWB pulse using time domain expressions. Since the interval of integration is very short compared to the duration of the baseband filter response, we can substitute the following approximate expression in the convolution integrals in (2a) and (2b):

$$h_0(t - \tau) \approx h_0(t) + \tau \cdot \frac{h_0(t - NT) - h_0(t)}{NT} \doteq h_0(t), \quad 0 \leq \tau \leq NT \quad (10)$$

This approach gives the following in-phase quadrature response to the UWB pulse:

$$\begin{aligned} p_I(t) &\approx h_0(t) \int_0^{NT} d\tau g(\tau) \cos(\omega_c \tau + \varphi) \\ &= h_0(t) \int_{-\infty}^{\infty} d\tau g(\tau) \cos(\omega_c \tau + \varphi) \\ &= h_0(t) \left\{ \frac{1}{2} e^{j\varphi} \int_{-\infty}^{\infty} d\tau g(\tau) e^{j\omega_c \tau} + \frac{1}{2} e^{-j\varphi} \int_{-\infty}^{\infty} d\tau g(\tau) e^{-j\omega_c \tau} \right\} \\ &= h_0(t) \left\{ \frac{1}{2} e^{j\varphi} G(-\omega_c) + \frac{1}{2} e^{-j\varphi} G(\omega_c) \right\} \end{aligned} \quad (11)$$

Similarly, the following cross-quadrature response is found as

$$\begin{aligned} p_Q(t) &\approx -h_0(t) \int_0^{NT} d\tau g(\tau) \sin(\omega_c \tau + \varphi) \\ &= -h_0(t) \int_{-\infty}^{\infty} d\tau g(\tau) \sin(\omega_c \tau + \varphi) \end{aligned} \quad (A.3)$$

$$= h_0(t) \left\{ \frac{j}{2} e^{j\varphi} G(-\omega_c) - \frac{j}{2} e^{-j\varphi} G(\omega_c) \right\} \quad (12)$$

This approximation based on the time domain calculation is in perfect agreement with the one based on the frequency domain calculation.

Example: for $1/T = 4\text{GHz}$ and $f_c = 5\text{GHz}$, the quadrature components of the N -cycle sinusoidal pulse are given by

$$p_I(t) \approx -(1.4 \times 10^{-10}) \sin(5N\pi/4 + \varphi) \times \sin(5N\pi/4) h_0(t)$$

and

$$p_Q(t) \approx -(1.4 \times 10^{-10}) \cos(5N\pi/4 + \varphi) \times \sin(5N\pi/4) h_0(t)$$

A plot of $p_I(t)$ for this numerical example is shown in Figure 3, assuming a narrowband signal data rate of $1/T_d = 20\text{MHz}$ and an ideal (rectangular) lowpass filter.

5. ESTIMATED RISE IN RECEIVER NOISE LEVEL

Using the foregoing methodology, the response of a narrowband direct conversion receiver to the UWB signal in (1), expressed using complex notation, is the interference waveform given by (1) with $g(t)$ replaced by $p_I(t) + jp_Q(t)$. I and Q UWB interference waveforms are given by

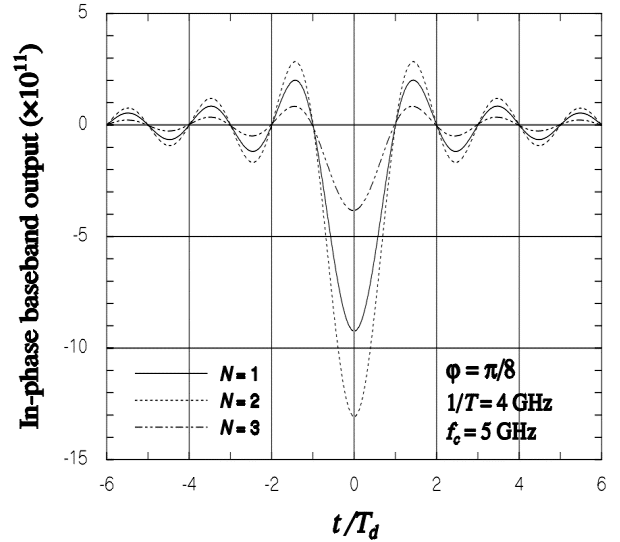


Figure 3. Numerical example of baseband response to UWB pulse.

$$z_I(t) = A_R \sum_{l=-\infty}^{\infty} u_l p_I(t - lT_u) \quad (13a)$$

$$z_Q(t) = A_R \sum_{l=-\infty}^{\infty} u_l p_Q(t - lT_u) \quad (13b)$$

where A_R is the received amplitude of the UWB pulse. These expressions are typical for cyclostationary data communication waveforms [7], except that a number of baseband interference pulses overlap at a given time, depending on the UWB signal's pulse rate.

Note that, since the bandwidth of the response to the UWB pulses at baseband is just the bandwidth of the receiver, a simulation of the UWB interference does not need to use the very high sampling rate that would be required to reproduce the unfiltered UWB pulse waveform.

Given the phase φ , the average power (variance) of the I-component of the UWB interference is

$$\sigma_I^2(\varphi) = A_R^2 \operatorname{Re}^2 \{ e^{-j\varphi} G(\omega_c) \} \sigma_u^2 X$$

where σ_u^2 is the variance of the UWB modulation symbols and

$$X = \frac{1}{T_u} \int_{-T_u/2}^{T_u/2} \sum_{l=-\infty}^{\infty} h_0^2(t - lT_u) dt = \frac{1}{T_u} \int_{-\infty}^{\infty} h_0^2(t) dt \quad (14)$$

By Parseval's theorem [8, 9], the integral in (14) equals the area in the frequency domain under the curve $|H_0(\omega)|^2$, which by definition equals $|H_0(0)|^2$ times the equivalent rectangular (noise) bandwidth of the filter, B_N . Thus we have

$$\sigma_I^2(\varphi) = \frac{1}{T_u} A_R^2 \operatorname{Re}^2 \{ e^{-j\varphi} G(\omega_c) \} \sigma_u^2 |H_0(0)|^2 B_N \quad (15)$$

This expression is conditioned on the oscillator phase, which can be expected to vary for different instances of UWB transmissions. Therefore it is reasonable to average it over the assumed uniform distribution of the phase. To perform this average, we note that

$$\begin{aligned} E_{\varphi} \{ \operatorname{Re}^2 \{ e^{-j\varphi} G(\omega_c) \} \} &= E_{\varphi} \left\{ \left| \operatorname{Re} \{ e^{-j\varphi} G(\omega_c) \} \right|^2 \right\} \\ &= \frac{1}{2} |G(\omega_c)|^2 = E_{\varphi} \{ \operatorname{Im}^2 \{ e^{-j\varphi} G(\omega_c) \} \} \end{aligned} \quad (16)$$

Therefore, the unconditional variance of the UWB interference in both I and Q quadratures of the receiver baseband is given by

$$\sigma_I^2 = \sigma_Q^2 = \frac{A_R^2}{2T_u} |G(\omega_c)|^2 \sigma_u^2 |H_0(0)|^2 B_N \quad (16)$$

This quantity can be compared with the variance of the receiver noise samples, which equals $N_0 B_N$, so the equivalent rise in the noise spectral density of the

receiver due to the UWB interference is (16) divided by the bandwidth.

Note that the expression for the UWB interference power in (16) accounts for the number of UWB pulses per data symbol of the affected communication system because it is proportional to the UWB pulse rate.

6. CONCLUSION

A methodology was shown for evaluating or simulating the effects of UWB pulsed communication waveforms on narrowband direct conversion receivers. The theoretical results in this paper establish a reference with which to compare simulation results. Further work on this topic that is needed include:

- *Statistical characterization of the net UWB interference at baseband by theory and simulation.* In this paper we have analyzed the power levels only.
- *Inclusion of multipath effects.* Since UWB pulse arrivals are very often accompanied by multipath, the UWB interference power in (16) should be increased by some factor to reflect the characteristics of the multipath environment that pertains to the coexistence scenario. Methods for determining such a factor are the subject of further research on this topic.

REFERENCES

- [1] P. Withington, "Ultra-wideband RF—A Tutorial," presentation to the IEEE 802 Plenary meeting in Albuquerque, March 2000. Document IEEE 802.15-00/083r0. Available online at <http://grouper.ieee.org/groups/802/15/pub/2000/Mar00/>
- [2] ——. First Report and Order in the matter of Revision of Part 15 of the Commission's Rules Regarding Ultra-Wideband Transmission Systems, Federal Communication Systems document FCC 02-48, 22 April 2002.
- [3] R. A. Scholtz, "Multiple Access with Time-Hopping Impulse Modulation," *Proc. IEEE 1993 Milit. Comm. Conf.*, pp. 457-450.
- [4] ——. "Propagation Measurement," web page of Ultra-Lab at the University of Southern California: http://ultra.usc.edu/New_Site/propagations.html
- [5] L. B. Michael, M. Ghavami, and R. Kohno, "Multiple Pulse Generator for Ultra-Wideband Communication using Hermite Polynomial Based Orthogonal Pulses," *Proc. UWBST 2002*, 21-23 May 2002, Baltimore.
- [6] L. E. Miller, "Autocorrelation Functions for Hermite-Polynomial Ultra-wideband Pulses," *IEE Electronics Letters*, Vol. 39, No. 11, pp. 870-871 (29 May 2003).
- [7] J. G. Proakis, *Digital Communications* (4th ed.). New York: McGraw-Hill, 2001.
- [8] J. S. Lee and L. E. Miller, *CDMA Systems Engineering Handbook*. Boston: Artech House, 1998.
- [9] B. P. Lathi, *Linear Systems and Signals*. Carmichael, CA: Berkeley-Cambridge Press, 1992.